

Determining Excitation-Energy Transfer Times and Mechanisms from Stochastic Time-Dependent Density Functional Theory

D. Hofmann-Mees¹, H. Appel^{2,3,4}, M. Di Ventura³, and S. Kümmel^{1*,†}

¹ *Theoretical Physics IV, University of Bayreuth, D-95440 Bayreuth, Germany,* ² *Fritz-Haber-Institut der Max-Planck-Gesellschaft, Faradayweg 4-6, D-14195 Berlin, Germany,* ³ *Department of Physics, University of California San Diego, La Jolla, CA 92093, USA, and* ⁴ *European Theoretical Spectroscopy Facility*

E-mail: stephan.kuemmel@uni-bayreuth.de;Phone:+49921553220

*To whom correspondence should be addressed

†¹ Theoretical Physics IV, University of Bayreuth, D-95440 Bayreuth, Germany

‡² Fritz-Haber-Institut der Max-Planck-Gesellschaft, Faradayweg 4-6, D-14195 Berlin, Germany

¶³ Department of Physics, University of California San Diego, La Jolla, CA 92093, USA

§⁴ European Theoretical Spectroscopy Facility

Abstract

We developed an approach for calculating excitation-energy transfer times in supermolecular arrangements based on stochastic time-dependent density functional theory (STDDFT). The combination of real-time propagation and the stochastic Schrödinger equation with a Kohn-Sham Hamiltonian allows for simulating how an excitation spreads through an assembly of molecular systems. The influence that approximations, such as the dipole-dipole coupling approximation of Förster theory, have on energy-transfer times can be checked explicitly. As a first application of our approach we investigate a light-harvesting inspired model ring system, calculating the time it takes for an excitation to travel from one side of the ring to the opposite side under ideal and perturbed conditions. Among other things we find that completely removing a molecule from the ring may inhibit energy transfer less than having an energetically detuned molecule in the ring. In addition, Förster’s dipole coupling approximation may overestimate excitation-energy transfer efficiency noticeably.

Keywords: light-harvesting, decoherence, Förster transfer, chromophore coupling,

1 Introduction

Electronic excitation-energy transfer (EET) after light absorption is one of the key processes in the natural light-harvesting (LH) event and a prerequisite for charge generation in the LH reaction center.^{1,2} Hence, it enables efficient energy recovery in biological systems. The efficiency of the light-harvesting process is determined by the rates of charge transfer and EET of many single transfer steps that all contribute to the overall mechanism. In multichromophoric supermolecules such as LH systems, the rates are affected by a number of different properties and phenomena: the electronic structure of the single chromophores, the electronic coupling between different system components, the geometry and arrangement of all constituents, the energetic and position (dis)order, and the interplay with the environment.

Recent years have seen an intense debate about the importance of intrinsic quantum mechanical effects for the LH process,^{3–6} specifically the existence of long-lived quantum coherences.^{7–9} The

character of these coherences, e.g., their electronic or vibronic nature, is still controversial.^{10,11} Quantum-coherence effects have also been found in artificial π -conjugated polymers.^{12,13} It has been argued that quantum-mechanical interference between different energy-transfer pathways may improve the efficiency of intrachain energy migration.¹² Thus, understanding the design of natural light-harvesting complexes may guide the future design of artificial organic devices.^{8,14,15}

Coherent energy transfer and the role of a system's environment can theoretically be studied using the density-matrix formalism. The models of Haken and Stobl, the model of Redfield, polaron modifications, or related theories have been employed.^{5,16–22} These concepts typically rely on input from electronic-structure theory or experiment. In the present work we present an alternative approach that addresses the energy-transfer problem directly at the level of electronic-structure theory by employing stochastic time-dependent density functional theory (STDDFT)^{23–31} which is an extension of standard time-dependent density functional theory (TDDFT) in real time,^{32–37} specifically formulated for open quantum systems.

Using TDDFT appears promising because it allows for calculating the electronic structure, the excitations, and also the couplings between the constituents of a supermolecular structure in principle exactly. TDDFT in practice can address multichromophoric systems of experimental relevance at a first-principles level at reasonable computational costs. The price one has to pay are the limitations of the available approximations for the exchange-correlation potential on which the predictive power of TDDFT calculations strongly depends. Luckily, in many energy-transfer situations long-range exchange and correlation (xc) do not play a decisive role as the intermolecular separations are large.^{38,75} Furthermore, recent progress in developing density functionals that can even describe charge-transfer situations reliably also allows for accurately describing excitations of complicated nature in complex systems.^{39–48} TDDFT with modern functionals thus appears as an ideal tool for studying energy-transfer processes on a first-principles basis.

However, there is still a conceptual hurdle that must be overcome. In most situations of interest the electronically active parts of a system interact with an environment, e.g., the phonons of a solvent or matrix. Taking all these degrees of freedom explicitly into account in a TDDFT calculation

is presently computationally impossible, and will probably be so for years to come. Therefore, an effective description that traces out the environment degrees of freedom is highly desirable. However, standard TDDFT is formulated using the closed quantum-system time-dependent Kohn-Sham (TDKS) equations that evolve coherently in time. In order to investigate the real-time dynamics of a system in contact with a dissipative bath one needs to go beyond standard TDDFT. Using open quantum-system schemes^{23–31,49–55} is an attractive option. The real-time TDDFT scheme for investigating EET processes that we present here employs the stochastic TDKS equations.^{23–28} We introduce a pragmatically motivated effective bath operator that couples to the dipole moment of the supermolecule or appropriate subsystems. As a first demonstration of our scheme we investigate a ring configuration of model molecules that is schematically inspired by nature’s circular LH complexes. We examine how different ways of treating the intermolecular coupling, e.g., using Förster’s dipole coupling approximation or not, and how energetic disorder influence energy-transfer times. In this first study we use the bath operator for determining the time that an excitation takes to spread in the system.

The paper is organized as follows. In 2 and the corresponding A we outline the stochastic TDKS approach and introduce a bath operator that couples to the dipole moment. Our ring-like model system is introduced in 3. In this section we also test the bath operator and explain the idea of using it for determining the effective time that an excitation travels in a supermolecular system. In 4 we report how variations in the electronic structure and how different intermolecular coupling mechanisms influence EET times. A summary and conclusions are offered in 5. Finally, B and C provide technical details about our electronic structure setup and our method for extracting coupling strengths from real-time TDDFT, respectively.

2 Dissipation in real-time time-dependent density functional theory

2.1 Stochastic Schrödinger equation

It is one of the basic ideas of open quantum-system approaches to split the entire Hamiltonian into system, bath, and system-bath interaction contributions, i.e.,

$$\hat{H} = \hat{H}_S \otimes \hat{I}_B + \hat{I}_S \otimes \hat{H}_B + \lambda \hat{H}_{SB}. \quad (1)$$

\hat{I}_S and \hat{I}_B denote identity operators in the system (S) and bath (B) Hilbert spaces. The system includes all dynamics and observables of, e.g., one molecular complex. The bath and system-bath coupling describe the environment, e.g., other surrounding molecules, and their interactions with the system. The system degrees of freedom can thus be coupled to a bosonic environment. The system itself is described by the electronic many-particle Hamiltonian

$$\begin{aligned} \hat{H}_S = \sum_i \left[\frac{[\hat{\mathbf{p}}_i + e\hat{\mathbf{A}}_{\text{ext}}(\hat{\mathbf{r}}_i, t)]^2}{2m} + \hat{v}_{\text{ext}}(\hat{\mathbf{r}}_i, t) \right] \\ + \sum_{i < j} \hat{W}(\hat{\mathbf{r}}_i - \hat{\mathbf{r}}_j), \end{aligned} \quad (2)$$

where \mathbf{A}_{ext} is an external vector potential, v_{ext} a scalar external potential, and \hat{W} describes the particle-particle interaction. The environment, represented by \hat{H}_B , induces a fluctuating force that drives the system via the system-bath interaction

$$\hat{H}_{SB} = \sum_{\alpha} \hat{S}_{\alpha} \otimes \hat{B}_{\alpha}. \quad (3)$$

This interaction is expressed in terms of many-particle operators \hat{S}_{α} and \hat{B}_{α} , where \hat{S}_{α} operates on the system degrees, \hat{B}_{α} on the bath degrees of freedom, and α denotes different possible system-bath coupling mechanisms. The bath may have a complex structure and not all of its microscopic

details are relevant for the system dynamics. The driving force that is induced by the bath may, therefore, be subsumed by stochastic fluctuation and dissipation contributions that can usually be characterized by mean values and correlation functions.⁵⁷ The parameter λ determines the strength of the system-bath interaction and can be used as an expansion parameter in the weak-coupling regime.

The dynamics of a quantum system in contact with an external bath can be described^{27,28,56–60} either by quantum master equations or by the stochastic Schrödinger equation (SSE). The latter uses a statistical ensemble of state vectors to represent the open quantum-system dynamics directly on the level of wave functions.

Throughout this work we use the SSE in the Born-Markov limit^{27,28,56–60}

$$\begin{aligned} i\partial_t\Psi_S(t) = & \hat{H}_S(t)\Psi_S(t) - \frac{i}{2}\sum_{\alpha}\hat{S}_{\alpha}^{\dagger}\hat{S}_{\alpha}\Psi_S(t) \\ & + \sum_{\alpha}l_{\alpha}(t)\hat{S}_{\alpha}\Psi_S(t), \end{aligned} \quad (4)$$

where $l_{\alpha}(t)$ are stochastic processes with vanishing ensemble average and δ -time-correlation

$$\overline{l_{\alpha}(t)} = 0, \overline{l_{\alpha}(t)l_{\beta}(t')} = 0, \overline{l_{\alpha}^*(t)l_{\beta}(t')} = \delta_{\alpha\beta}\delta(t-t'). \quad (5)$$

The bar denotes the statistical average over an ensemble of stochastic processes. For the sake of convenience the coupling strength parameter λ here has been absorbed into the bath operator \hat{S}_{α} . The first term of the SSE (??) determines the usual unitary system evolution under the action of the system Hamiltonian \hat{H}_S . Although the SSE employs the system Hilbert space only, the coupling to the bath is still included by the second term that describes dissipation effects due to the system-bath interaction. Finally, the third term introduces fluctuations in the time evolution: Although the dissipative term causes the probability density to decay in time, the norm of the state vector $\Psi(t)$ averaged over a statistical ensemble of realizations is conserved up to fourth order in the system-bath coupling parameter λ . In the following, we focus on a single bath operator \hat{S} and can thus omit the index of the bath operator.

As a result of the stochastic nature of (??) the system wave function can not be simulated by a single evolution of the SSE but needs to be represented by a statistical ensemble of wave functions $\{\Psi_s(t)\}$. Accordingly, starting from a pure initial state, the full time evolution of expectation values

$$\overline{O_S}(t) = \overline{\langle \hat{O}_S \rangle} = \overline{\langle \Psi(t) | \hat{O}_S | \Psi(t) \rangle} \quad (6)$$

of physical observables needs to be calculated from the statistical average over all ensemble members as indicated by the bar. A reliable computation of smooth observables requires a large enough set of stochastic realizations.

Working with the SSE tremendously reduces the complexity of the problem one has to solve. However, it introduces the question of choosing appropriate bath operators and it does not answer the question of how to describe the system itself (\hat{H}_S). In the following we first address the latter question and then the former.

2.2 Stochastic Schrödinger equation and Kohn-Sham density functional theory

It has been shown that the open quantum-system SSE approach can be combined with TD current density functional theory (TDCDFT),^{23,24} and the applicability of the approach has been discussed in Refs.^{26–28} In contrast to standard TD(C)DFT, the open quantum-system approach operates on ensemble-averaged quantities. It requires the ensemble-averaged particle density

$$\overline{n(\mathbf{r}, t)} = \overline{\langle \hat{n}(\mathbf{r}) \rangle}, \quad (7)$$

where the density operator is defined as

$$\hat{n}(\mathbf{r}) = \sum_i \delta(\mathbf{r} - \hat{\mathbf{r}}_i), \quad (8)$$

and the ensemble-averaged current density

$$\overline{\mathbf{j}(\mathbf{r}, t)} = \overline{\langle \hat{\mathbf{j}}(\mathbf{r}, t) \rangle}, \quad (9)$$

where the current operator reads

$$\hat{\mathbf{j}}(\mathbf{r}, t) = \frac{1}{2} \sum_i \left\{ \delta(\mathbf{r} - \hat{\mathbf{r}}_i), \frac{\hat{\mathbf{p}}_i + e\hat{\mathbf{A}}_{\text{ext}}(\hat{\mathbf{r}}_i, t)}{m} \right\} \quad (10)$$

and $\{.,.\}$ denotes the anticommutator bracket. The KS Hamiltonian reads

$$\begin{aligned} \hat{H}_{\text{KS}} = \sum_i \left[\frac{[\hat{\mathbf{p}}_i + e\hat{\mathbf{A}}_{\text{ext}}(\hat{\mathbf{r}}_i, t) + e\hat{\mathbf{A}}_{\text{xc}}(\hat{\mathbf{r}}_i, t)]^2}{2} \right. \\ \left. + \hat{v}_{\text{ext}}(\hat{\mathbf{r}}_i, t) + \hat{v}_{\text{H}}(\hat{\mathbf{r}}_i, t) \right], \end{aligned} \quad (11)$$

with the external vector potential $\mathbf{A}_{\text{ext}}(\mathbf{r}, t)$, the xc vector potential $\mathbf{A}_{\text{xc}}(\mathbf{r}, t)$, and the Hartree potential $v_{\text{H}}(\mathbf{r}, t)$. The xc vector potential in the open quantum-system approach may in general depend on $\overline{\mathbf{j}(\mathbf{r}, t)}$, the initial state $\Phi_{\text{KS}}(\mathbf{r}, t = 0)$, and the bath operator \hat{S} . The system dynamics can be calculated from the KS Slater determinant $\Phi_{\text{KS}}(\mathbf{r}, t)$ evolving according to the open system KS equation²³

$$i\partial_t \Phi_{\text{KS}}(t) = \hat{H}_{\text{KS}} \Phi_{\text{KS}}(t) - \frac{i}{2} \hat{S}^\dagger \hat{S} \Phi_{\text{KS}}(t) + l(t) \hat{S} \Phi_{\text{KS}}(t). \quad (12)$$

For practical calculations one needs to rely on existing approximations for the xc vector potential as the true $\mathbf{A}_{\text{xc}}(\mathbf{r}, t)$, especially in open quantum systems, is not known.²³

Practical applications of stochastic TDDFT so far rely on approximate realizations of the stochastic formalism in KS TDDFT instead of TDCDFT. In Refs.^{25,26} the system Hamiltonian is approximated by a standard TDDFT Hamiltonian

$$\hat{H}_{\text{KS}} = \sum_i \left[\underbrace{-\frac{\hat{V}_i^2}{2} + \hat{v}_{\text{ext}}(\hat{\mathbf{r}}_i, t) + \hat{v}_{\text{H}}(\hat{\mathbf{r}}_i, t) + \hat{v}_{\text{xc}}(\hat{\mathbf{r}}_i, t)}_{=:\hat{h}_{\text{KS}}(\hat{\mathbf{r}}_i, t)} \right] \quad (13)$$

and used in the open quantum-system KS equation (??) together with a heuristic bath operator.³⁰ Here, we apply an open quantum-system KS scheme of the same pragmatic kind. Exchange and correlation are described by the adiabatic local density approximation. A detailed discussion of the difficulties of establishing a DFT Hamiltonian in the open quantum-system framework, addressing, e.g., issues such as the v -representability problem of the current density,⁶³ is given in.⁶⁴

Going over to standard TDDFT and letting bath operators act on the TD KS states implies possibly far reaching approximations, because neither is the KS wavefunction necessarily a good model for the true wavefunction, nor is it clear that xc effects in the system-bath couplings can be neglected. With respect to the first issue there is some hope that at least for many organic systems that are of interest in the light-harvesting context the approximation is not too bad, because the wavefunction of many organic semiconductors is dominated by a single Slater determinant.⁶⁵ This is reflected, e.g., in angular resolved photoemission experiments that reveal very clear signatures of single molecular orbitals.^{66,67} Also for the model dimers that we study in this paper correlation is weak and one can hope that it is not too unrealistic to rely on the KS states. Evaluating the second issue, i.e., the importance of a more complete description of the system bath xc coupling, goes beyond the aims of the present manuscript in which the focus lies on exploring a transparent, pragmatically motivated bath operator that is described in the next section.

2.3 The bath operator

The choice of the bath operator is the second ingredient needed for defining the open quantum-system scheme. Our aim is a bath operator that introduces dissipation by taking the excited quantum system back to its ground state. Thus, we define the bath operator as a projector of the form

$$\hat{S} = \sqrt{\gamma}M[n(\mathbf{r},t)]|\Phi_{\text{KS}}(t_0)\rangle\langle\Phi_{\text{KS}}(t)|. \quad (14)$$

It includes two scaling factors $\sqrt{\gamma}$ and $M[n(\mathbf{r},t)]$. Choosing $M = 1$ would amount to a de-excitation of the entire system with a decay rate γ and a decay time constant $\tau = 1/\gamma$.

The aim of our present study is to explore the possibilities that the open quantum-system KS equations offer in the field of molecular excitation-energy transfer. With a density-dependent factor $M[n(\mathbf{r},t)]$, the bath operator (??) allows for modeling a broad range of physical situations that can be of relevance in this context. Here we specifically want to investigate a dissipation mechanism that depends on the (transition) dipole moment of the excited system, i.e., we want to choose M proportional to the time variation of the dipole moment $\mathbf{d}(t) = \int \mathbf{r}n(\mathbf{r},t) d^3r$: $M[n(\mathbf{r},t)] \propto |\mathbf{d}(t) - \mathbf{d}(t_0)|$. This form of the bath operator is not derived ab initio, but is motivated from physical considerations. We are here thinking about describing situations where several subsystems (e.g. several chromophores) can exchange energy with each other and with a surrounding environment (e.g. a matrix embedding the chromophores). When a subsystem is strongly excited (indicated by a large induced dipole moment) it should transfer more energy to the environment than a weakly excited subsystem. The operator M deliberately models only the system part of the system-bath interaction as the bath side of the coupling mechanism is subsumed in the effective decay rate. An accurate description of chromophore-matrix interactions in future work may of course need to employ more sophisticated bath operators, but in this first exploratory study here we want to test whether the transparent, dipole-dependent mechanism can be realized.

2.4 Simulation algorithm

Having introduced the stochastic TDDFT formalism and a model bath operator, we finally turn our attention to the practical algorithm that we use to solve the open system KS equations. Our simulations are conducted with the quantum-jump algorithm^{56,58,68,69} that has been introduced in the context of open quantum-system KS equations in Ref.²⁶ The algorithm is implemented in the Bayreuth version⁷⁰ of the PARSEC real-space program package⁷¹ and rests upon the single-particle bath operator

$$\hat{s}_i = \sqrt{\gamma}M[n(\mathbf{r},t)]|\varphi_i(t_0)\rangle\langle\varphi_i(t)|. \quad (15)$$

We demonstrate in A that using this bath operator in the following set of quantum-jump single-particle equations is equivalent to using \hat{S} in the corresponding algorithm for solving (??). The quantum-jump algorithm relies on a piecewise deterministic evolution^{26,58} of the set of norm-preserving Schrödinger equations

$$i\partial_t \varphi_i(t) = \hat{h}_{\text{KS}} \varphi_i(t) - \frac{i}{2} \hat{s}_i^\dagger \hat{s}_i \varphi_i(t) + \frac{i}{2} |\hat{s}_i \varphi_i(t)|^2 \varphi_i(t), \quad (16)$$

that are interrupted by quantum jumps. The quantum jumps represent the non-deterministic action of the bath operator. Occurrence of a quantum jump at a given time means that at this time the bath operator transfers the system to a different state according to its projector part. Here, the TD orbitals are transferred to the corresponding ground-state orbitals. The points of time where such a jump occurs are determined by a random process according to a waiting-time distribution. However, as this waiting-time distribution is not known beforehand, it needs to be determined alongside the actual propagation of the open quantum KS system (for details, see Ref.²⁶): The waiting-time distribution is determined from the decay of the norm

$$\eta(t) = \frac{1}{N} \sum_i \int |\varphi_i^{\text{aux}}(\mathbf{r}, t)|^2 d^3 r \quad (17)$$

of an auxiliary system of N particles evolving according to the non-norm conserving equation

$$i\partial_t \varphi_i^{\text{aux}}(t) = \hat{h}_{\text{KS}} \varphi_i^{\text{aux}}(t) - \frac{i}{2} \hat{s}_i^\dagger \hat{s}_i \varphi_i^{\text{aux}}(t). \quad (18)$$

One obtains a single waiting time by drawing a random number in the interval $[0,1]$ and choosing as the quantum-jump time the time T at which $\eta(T)$ drops below this number. The waiting-time distribution is then calculated from many of such single jump times.

In this algorithm our choice of bath operator leads to an additional beneficial property. When no additional external perturbations act after the initial excitation, the bath mechanism relaxes the system to its ground state, and the system remains in the ground state after each quantum jump.

Therefore, the time evolution of all members of the stochastic ensemble follows the same pattern: The KS system first evolves deterministically until a quantum jump occurs and then – after the system has jumped back to the ground state – the KS orbitals propagate trivially with TD phases following from the ground-state KS eigenvalues. Therefore, the full statistical ensemble can be generated from a single deterministic evolution of (??) alongside with the determination of the waiting-time distribution. The complete simulation therefore proceeds as follows: (i) Calculate a long enough deterministic evolution together with the norm decay of the auxiliary system, i.e., solve Eqs. (??) and (??). (ii) Draw a large number of random numbers, find the corresponding quantum-jump times, and determine the waiting-time distribution. (iii) For each quantum-jump time construct the corresponding trajectory by combining the time evolution as calculated in step (i) (used for the times smaller than the jump time) with ground-state values (used for the times larger than the jump time). (iv) Calculate the physical quantities of interest by averaging (cf. (??)) the observables over the ensemble of trajectories that has been obtained in step (iii).

As an aside we note that an explicit orthogonalization of the orbitals as done in Ref.²⁶ is not needed here because the bath operator preserves the orthogonality of the KS orbitals.

3 Model system and bath coupling mechanism

3.1 Model setup

In the following we use the approach that we introduced in the previous sections for investigating energy transfer in a model system of circularly arranged molecules. The geometric arrangement of the molecules is designed to schematically resemble circular LH complexes of the antenna system of LH organisms. Our aim is to study the influence of electronic-structure properties on the EET time scales and pathways in such supermolecules. In this first study we focus on the influence of the coupling between the molecules that build the supermolecule.

The setup consists of eight equidistantly spaced molecules, see 1. Starting from the ground state we excite one of the molecules, in the following labeled m5. This excitation of the one

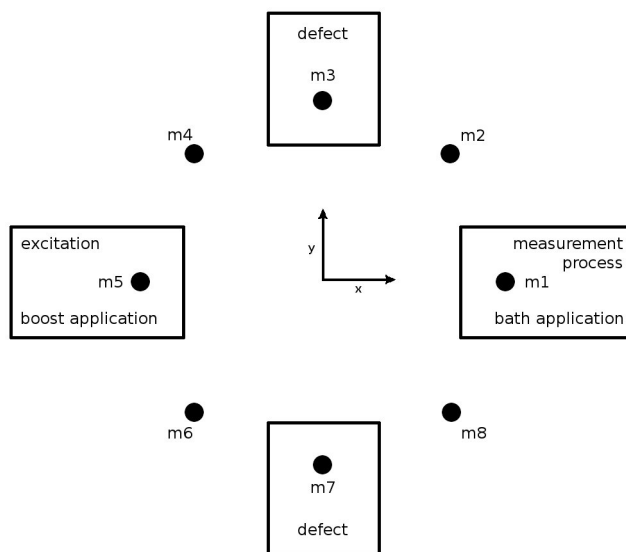


Figure 1: Schematic illustration of the ring-like model system consisting of eight individual molecules m_1, m_2, \dots, m_8 . We determine how excitation energy spreads from m_5 to m_1 as described in the main text. For investigating the effects of changes in the intermolecular coupling we introduce defects in the molecules m_3 and m_7 . See B for further details.

molecule m_5 is numerically realized by applying the boost excitation that is described below only to the (45-degree) sector of the grid that is associated with m_5 . In other words, all eight molecules are placed on the same large three-dimensional grid during the simulation, but for excitation and bath action we associate each molecule with a certain part of the grid, namely the 45-degree sector in which it lies.

We simulate the excitation by a momentum boost of the type that is frequently used in real-time TDDFT.^{34,35,72–74} The boost has dipole character, and this conforms with our aim of modeling optical dipole excitations. However, whereas the external potential for a laser excitation (assuming a classical, non-quantized electromagnetic field) would correspond to a TD oscillating dipole potential with a TD envelope function, the boost is instantaneous. It can be understood as a “spectrally absolutely broad” excitation that can couple to all eigenfrequencies of a system and is therefore not a model for a laser field. However, for the purposes of our present study we deliberately choose this type of excitation because it allows for a precise definition of the time at which the excitation begins and a corresponding definition of an energy-transfer time. Furthermore, in the model system that we study here the spectrum of an individual molecule for a given excitation-polarization

direction is strongly dominated by a single excitation. Therefore, the boost can be interpreted as instantaneously populating this one excited state. The dynamics that is triggered when the boost is applied to one molecule can therefore be seen as an approximation to the situation that the molecule is initially transferred into an excited state by absorption of a photon. We also stress that the computational approach that we present here is not tied to the boost excitation, and other, explicitly time-dependent excitations can be used as well.

Because we want to measure excitation-energy transfer from m5 to m1 we design an operator of the form (??) such that it couples to variations of the dipole moment $|\mathbf{d}_1(t) - \mathbf{d}_1(t_0)|$ of molecule m1 only. The index indicates that the dipole moment is calculated only in the (45-degree) section of the grid corresponding to m1. The bath operator projects onto the ground state and thus removes the entire excitation energy. This model is to be understood as an averaging approximation to a more realistic de-excitation mechanism in which the energy would dissipate to many lower energy levels. The scaling factor M in the bath operator includes a normalization factor D and reads

$$M[n(\mathbf{r},t)] = \frac{|\mathbf{d}_1(t) - \mathbf{d}_1(t_0)|}{D}. \quad (19)$$

So far the time constant related to the rate of the dissipative mechanism is a free parameter, whereas D needs to be chosen reasonably as discussed below in 3.2. In summary, the bath mechanism measures locally the amount of excitation energy that has reached m1 and de-excites the entire system accordingly. The motivation for this concept will be further explained below.

In this first study our focus is on establishing our approach and on a transparent analysis of the influence of the intermolecular coupling mechanism. Therefore, although our setup is suitable for general chromophores in a ring-like arrangement, we here choose dimers as the components of the circular system (see B). For these the electronic structure, e.g., excited-state energies, can easily be modified by bond-length variation. In this way, defects can be introduced in a well controlled way. For a transparent analysis we modify only molecules m3 and m7 in our investigations in 4 and fix all other system components, see 1. The electronic-structure properties of the model system are

discussed in detail in B.

In a circular arrangement of model molecules there are at least three sources for relevant time scales: time scales related to the energy of the individual molecular excited states, time scales due to the intermolecular coupling (here, more than one time scale is involved if the system is partly or totally off-resonant), and time scales due to the dissipative bath action. The first two types of time scales are determined by the molecular setup and system-internal interactions. The related dynamics are accessible in closed quantum-system simulations. Yet, for computing the energy-transfer dynamics of a system interacting with its environment, i.e. also taking the latter type of time scales into account, open quantum-system schemes as the one presented here are needed. We emphasize that Markovian system-bath couplings, as e.g. the one employed in the present approach, will only provide a damping mechanism which prevents excitation energy from coherently travelling throughout the system. Besides a small Lamb-Shift type correction induced by the Markovian system-bath coupling, no modifications of excitation-energy transfer times can be achieved in such a coupling limit. Non-Markovian system-bath couplings on the other hand will be capable of modifying excitation-energy transfer times. As shown in Ref.,⁵⁷ stochastic Schrödinger equations naturally allow to include Non-Markovian system-bath interactions. A natural next step beyond the present exploratory work is therefore to investigate Non-Markovian system-bath couplings within a stochastic TDKS approach.

Before we discuss the life-time of the excitation on the ring in 4, we first study the influence that the bath has on a single dimer.

3.2 Assessment of the bath operator

The aim of this section is to define D in such a way that the role of the scaling factors γ and $(|\mathbf{d}_1(t) - \mathbf{d}_1(t_0)|)/D$ that appear in front of the projector can be well separated: γ should set the decay time $\tau = 1/\gamma$, and the dipole dependent scaling factor should account for the coupling to the dipole moment of molecule m1 without interfering with the role of γ . Therefore, D needs to be adapted to the dipole oscillations of the isolated model molecule m1.

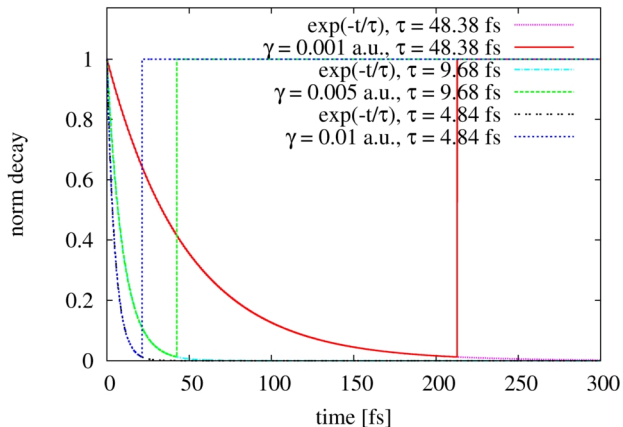


Figure 2: Norm decay $\eta(t)$ of a single model molecule. The damping is performed with different decay-time constants τ after an initial boost excitation with 0.001 eV excitation energy. The norm decay is always exponential $\exp(-t/\tau)$ with the preset time τ . Here, quantum jumps were performed as the norm dropped below 0.014 %. They are seen as vertical lines leading back to a norm of one.

To determine D we calculated 100 fs of the dipole-moment time evolution of a single molecule as a closed quantum system after an initial momentum boost along the bond axis of the dimer. Thus, only the dipole moment along this axis is excited and the investigation can be restricted to this dipole-moment component. *A priori* one can think of different options for computing D : It may be chosen to be, e.g., the first maximum, the average over all maxima, the absolute average, or the absolute square average of the dipole moment. We found by numerical tests that an exponential decay with the time constant τ is reached only when D is chosen as the average of the absolute square of the dipole moment. 2 shows the norm decay of the auxiliary system of the quantum-jump algorithm. For all cases studied, the actually observed decay is exponential with the preset decay rate, as desired.

Another factor that needs to be taken into account in setting up D is the energy of the boost excitation. The dissipation of energy should be independent of the boost strength. Therefore, we adapt the normalization factor to the boost strength by first determining D from a closed quantum-system calculation with the same initial boost excitation that we later use in the open quantum-system calculation. Our calculations show that the normalization factor thus obtained yields a decay time that is independent of the boost strength.

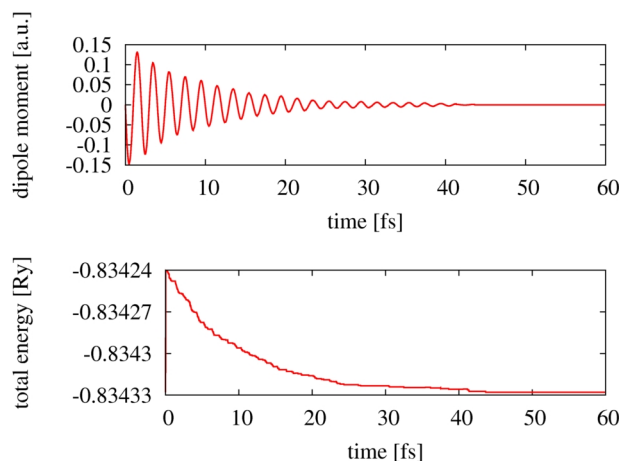


Figure 3: Ensemble-averaged dipole moment (z -component) and total energy of a single molecule in contact with a dissipative bath that induces a decay time of 10 fs. 200 realizations have been computed.

Having investigated the norm decay in detail, we finally give some results on other important observables. The exponential decay of the norm translates into an exponential decay of the total energy and the envelope of the dipole-moment oscillation (see 3). Thus, the bath operator fulfills all desired criteria.

4 Excitation-energy spread in a ring system

4.1 Resonant excitation spread and decay time constants

We now investigate EET in circular supermolecules and start by studying the perfectly resonant coupling situation, i.e., all molecules of the ring are identical. 4 shows the time evolution of the dipole moment of four molecules in the ring of 1. The dynamics here is fully coherent, i.e., there is no coupling to the bath. The initial excitation is a boost of $m5$ as explained in 3, and the intermolecular distance within the ring is 20 Bohr. We observe a fast oscillation of the dipole moment that corresponds to the lowest excitation energy of our model system at 2.1 eV, with an envelope that shows an interference pattern: At different points in time the largest dipole moment amplitude is observed on different subsystems. This interference pattern emerges as the dipolar excitation travels along the ring in both directions. It is governed by the intermolecular coupling

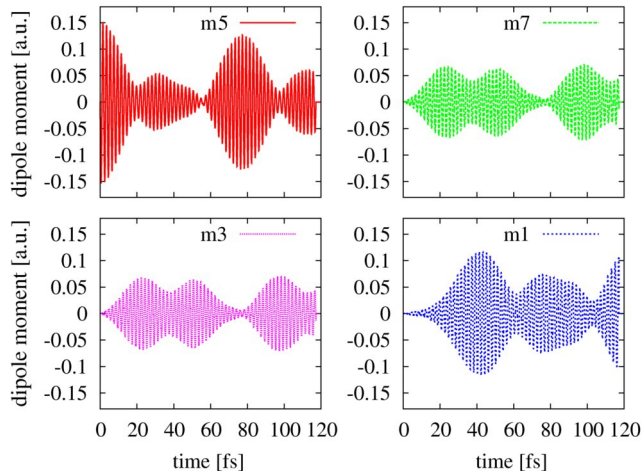


Figure 4: Dipole moment (z -component) of the four molecules $m1$, $m3$, $m5$, $m7$ in the ring system of 1. The intermolecular distance is 20 Bohr. At $t = 0$ $m5$ was excited by a boost with 0.001 eV excitation energy. In this simulation there is no dissipation. An oscillation pattern emerges due to interferences of the dipolar excitation that is traveling around the ring.

strength, i.e., the pattern is determined by the time an excitation needs to be transferred between neighboring molecules. For a separation of 20 Bohr the coupling strength is 0.038 eV in our model system.⁷⁵ If two of our model molecules were isolated, this coupling would amount to a resonance oscillation with a cycle duration of 107.8 fs and after each quarter of this period the maximum of the dipole oscillation would be observed on one of the two neighbors.⁷⁵ In the circular setup each molecule has neighbors on both sides and the excitation thus spreads through the ring.

When we now add the bath mechanism to measure the EET time the bath needs to break the coherence and thus needs to operate on a comparably short time scale. We choose a decay time of 5 fs, and this choice will be motivated further below. 5 shows the time evolution of the dipole moment of the same molecules as in 4. Due to the bath an additional time scale comes into play and one can clearly see how the oscillation of the dipole moment decays in all molecules due to the dissipative process. To be able to measure the traveling time of an excitation in the circular setup, the decay time needs to be chosen short enough to sample the initial stage of the coherent EET before the interference pattern starts to build up. In the example of 5, the decay time of 5 fs fulfills this criterion: The dipole oscillation at molecule $m1$ reaches only one maximum and subsequently decays to the ground state. Thus, no interference emerges.

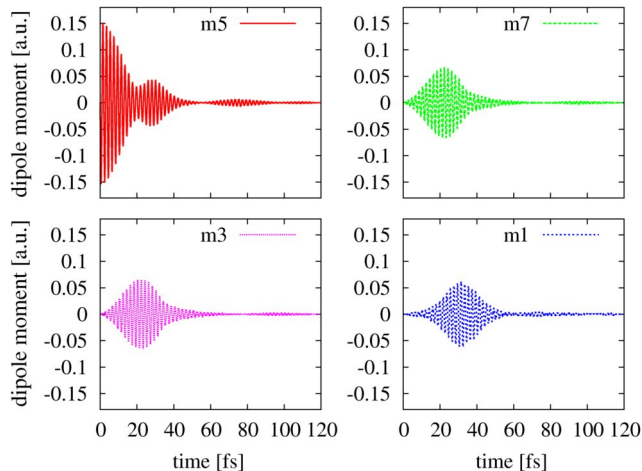


Figure 5: Ensemble-averaged (over 200 realizations) dipole moment (z -component) time evolution of four molecules that are arranged as in 4. After the initial excitation at m5 the excitation travels in the ring and decays due to a dissipative bath that is acting with a decay time of 5 fs on molecule m1.

We define the time that serves as our measure for how long an excitation needs for traveling from m5 to m1 via the decay of the norm η of the auxiliary system. The rationale behind this choice is the following: The bath operator is sensitive to the (transition) dipole moment of m1, i.e., energy departs the system relative to the amount of excitation energy that arrives at molecule m1. The energy loss of the system is measured by the decay of the norm of the auxiliary system. Therefore, η serves as measure for the excitation energy that reaches m1. In practice we choose a threshold value for η and monitor at which time T the norm η falls below this value. Depending on how large the chosen threshold is, the criterion can measure somewhat different effects. When the threshold is chosen relatively large (note that with a rapid norm decay as seen in 2 a value of 0.1 can be “large”), then the time T is determined by just the initial energy transfer and reflects how quickly energy spreads through a previously unexcited system. When the threshold is chosen smaller, than the criterion not only measures the initial energy transfer but also takes into account that the energy transfer can change as molecules on the way between m5 and m1 become excited. This way of defining energy-transfer times is not unique, but it appears reasonable on physical grounds. In our study we considered the norm decay down to three different thresholds, 0.100, 0.050, and 0.012. The first line of 1 lists the times T that we determined for the ring with all

molecules identical. These values serve as reference values for investigating how the excitation spread-time changes when defects are introduced into the ring.

4.2 Influence of energetic disorder

Table 1: Times T where the norm $\eta(T)$ of the decaying auxiliary system drops below 0.100, 0.050, and 0.012. The different lines correspond to different setups of the ring. We modified the ring by either varying the bond length and thus the excitation energies of m3 and m7, or by removing them completely, as indicated in the first two columns of the table. A bond-length reduction of 0.1 Bohr (0.5 Bohr) amounts to an energetic detuning of the excitation energy by 0.049 eV (0.135 eV), and a reduction of the coupling-matrix element by 0.006 eV (0.012 eV), respectively.

m3	m7	$\eta = 0.100$	$\eta = 0.050$	$\eta = 0.012$
0.0 Bohr	0.0 Bohr	52 fs	75 fs	117 fs
-0.1 Bohr	0.0 Bohr	56 fs	110 fs	121 fs
-0.5 Bohr	0.0 Bohr	84 fs	97 fs	143 fs
-0.1 Bohr	-0.1 Bohr	57 fs	112 fs	123 fs
-0.1 Bohr	-0.5 Bohr	85 fs	97 fs	157 fs
-0.5 Bohr	-0.5 Bohr	166 fs	181 fs	211 fs
removed	0.0 Bohr	80 fs	89 fs	125 fs
removed	-0.1 Bohr	99 fs	125 fs	147 fs
removed	-0.5 Bohr	205 fs	227 fs	265 fs

We assess the influence of energetic disorder on the EET time by introducing defects via bond-length variations and/or removing one of the molecules. The lower lines of 1 list the times T for the cases that a small (line 2) and a stronger energetic detuning (line 3) have been introduced in one arm of the ring, in both arms of the ring (lines 4 and 5), and with one molecule removed in one arm (lines 6 to 9). We find that small changes of the bond length (-0.1 Bohr) in m3 or in both m3 and m7 result in only a moderate increase of the transfer time. Larger increases are observed when a larger defect (-0.5 Bohr) is introduced in one of the molecules. The table also shows that interference effects have an influence on T : While the times corresponding to a decay down to $\eta = 0.100$ and $\eta = 0.012$ give a consistent picture, the situation is different for the times T corresponding to $\eta = 0.050$. Independent of this, however, there is a clear rise of the transfer time as soon as the more severe defect is introduced in both arms of the ring. In this case the life-time

of the excitation on the ring increases by about a factor of two.

Another type of defect can be introduced by removing a molecule (m3) from the ring. In this case the coupling between molecules m2 and m4 is about an order of magnitude smaller than the next-neighbor coupling between the other molecules.⁷⁵ The first interesting observation in this case is made by comparing line 7 of 1 (m3 removed) to line 3 (m3 disturbed): Detuning the excitation energy of m3 inhibits energy transfer more than removing m3 completely. The second observation is that energy transfer is seriously hindered when now also the other arm of the ring is disturbed by detuning molecule m7.

We summarize the findings by concluding that (i) interference effects play a role for the lifetime of the excitation on the ring, (ii) as soon as sizable defects occur in both pathways EET is hindered noticeably, whereas a defect in one pathway has less dramatic influences, (iii) for resonant or close-to-resonant cases the EET time is not affected much by variations of the coupling strength, and removing one subsystem of the ring hinders EET less than a sizeable energetic detuning of this subsystem.

4.3 Influence of the intra-system coupling

In the final investigation we examine how EET times change when the frequently employed⁷⁵⁻⁷⁷ dipole-coupling approximation of Förster theory is used instead of the full coupling. For our model system it is known⁷⁵ that the true coupling between two molecules differs noticeably from the dipole-dipole approximation for distances below 20 Bohr. Therefore, the intermolecular distance was reduced to 12 Bohr in the following calculations to model a situation in which the ring members are so close that the dipole approximation cannot be expected to be realistic. We implement the dipole-coupling approximation by a multipole expansion of the molecular interaction and truncating the latter after the dipole-dipole contribution. More details are described in Ref.⁷⁵ Here, we use Förster-type dipole-coupling between all molecules in the ring setup. The aim of this study is to check which conclusions one would (wrongly) draw when one assumes dipole coupling in a situation where the dipole approximation breaks down. The (full) coupling-matrix element at 12

Bohr is 0.105 eV,⁷⁵ i.e., notably larger than in the previous examples, but we kept the dissipation time constant at 5 fs.

Table 2: Compiled are the times T at which $\eta(T)$ drops below 0.100, 0.050, and 0.012 (columns 3, 4, and 5, respectively) for a ring with an intermolecular distance of 12 Bohr. Full coupling is compared to dipole-dipole coupling. The ring is disturbed via bond-length variations in molecule m3 as indicated in the second column.

coupling	m3	$\eta = 0.100$	$\eta = 0.050$	$\eta = 0.012$
full	0.0 Bohr	95 fs	116 fs	163 fs
Förster	0.0 Bohr	86 fs	104 fs	152 fs
full	-0.1 Bohr	99 fs	140 fs	182 fs
Förster	-0.1 Bohr	94 fs	108 fs	154 fs
full	-0.5 Bohr	109 fs	140 fs	209 fs
Förster	-0.5 Bohr	89 fs	115 fs	185 fs

2 shows the EET times that we determined as described above for an undisturbed ring and with perturbations on one side of the ring. In each case we ran a simulation once with full coupling and once with dipole-dipole coupling but otherwise identical parameters. The table shows that the Förster-type dipole coupling underestimates the times T in all cases, i.e., in our setup it overestimates EET efficiency. This finding is in line with the observation that the coupling-matrix element is overestimated by the dipole approximation.⁷⁵ A further interesting observation is that the times T here, i.e., for an intermolecular distance of 12 Bohr, are larger than the corresponding times for an intermolecular distance of 20 Bohr, although in the latter case the coupling is notably weaker. This may seem like a contradiction, but is a real effect caused by the interferences that are more pronounced in case of stronger coupling. Therefore, care has to be taken when comparing absolute times unless the dissipation time constant of the bath operator is chosen short enough to prevent a buildup of interferences due to excitation-energy spread along different available pathways.

5 Summary and Conclusions

In summary, we developed and used a stochastic TDDFT-based approach for open quantum systems to investigate the excitation-energy spread in a circular arrangement of molecules. We in-

roduced a bath operator that couples to the dipole moment of specific subsystems of the supermolecular complex. The dissipative mechanism breaks the coherent EET and removes excitation energy from the system. It allows for measuring energy-transfer times. The influence of electronic-structure properties and intermolecular coupling mechanisms on the EET process can thus be investigated. We demonstrated among other things that sizeable perturbations of the electronic structure of a model ring system lead to a considerable decrease in energy-transfer efficiency if both pathways of the ring are perturbed, completely removing a molecule from the ring can inhibit energy transfer less than having an energetically detuned molecule in the ring, and Förster’s dipole coupling approximation may overestimate EET efficiency noticeably. Our scheme is completely general and future applications can be extended to much more complex molecular setups than the one of this first study. The approach can therefore help to shed light onto the complex phenomena that govern one of nature’s most fascinating processes, the collection of light by plants and bacteria.

Financial support by the DFG Graduiertenkolleg 1640 is gratefully acknowledged by SK and DH, and DH also acknowledges the hospitality of the UCSD. MD acknowledges support from DOE grant DE-FG02-05ER46204.

A Single-particle representation of the bath operator

In this appendix we demonstrate that using the single-particle operator \hat{s}_i of (??) in the set of single-particle equations of 2.4 is equivalent to solving (??) with the bath operator \hat{S} of (??) using the quantum-jump algorithm. In the latter case, one needs to propagate simultaneously the norm-preserving equation

$$i\partial_t\Phi_{\text{KS}} = \hat{H}_{\text{KS}}\Phi_{\text{KS}} - \frac{i}{2}\hat{S}^\dagger\hat{S}\Phi_{\text{KS}} + \frac{i}{2}\|\hat{S}\Phi_{\text{KS}}\|^2\Phi_{\text{KS}} \quad (20)$$

and the auxiliary equation

$$i\partial_t\Phi_{\text{KS}}^{\text{aux}} = \hat{H}_{\text{KS}}\Phi_{\text{KS}}^{\text{aux}} - \frac{i}{2}\hat{S}^\dagger\hat{S}\Phi_{\text{KS}}^{\text{aux}}. \quad (21)$$

Inserting \hat{S} of (??) in (??) yields the closed quantum-system KS equation

$$i\partial_t\Phi_{\text{KS}} = \hat{H}_{\text{KS}}\Phi_{\text{KS}}. \quad (22)$$

The latter equation can be translated to the well-known set of single-particle KS equations that one also obtains by inserting \hat{s}_i of (??) into (??).

It remains to be checked that with our choice of bath operator the single-particle equation (??) indeed corresponds to the many-particle equation (??). To this end we use the method of Ref.⁷⁸ for deriving the single-particle equations that correspond to (??). We start from the reduced one-body density matrix

$$\begin{aligned} \rho(\mathbf{r}, \mathbf{r}', t) &= \int \Phi_{\text{KS}}(\mathbf{r}, \mathbf{r}_2, \dots, \mathbf{r}_N) \\ &\quad \Phi_{\text{KS}}^*(\mathbf{r}', \mathbf{r}_2, \dots, \mathbf{r}_N) d^3r_2 \dots d^3r_N \end{aligned} \quad (23)$$

and compute the equation of motion for it by inserting the open quantum-system KS equation and the specific form of (??) for \hat{S} to find

$$\begin{aligned} i\partial_t\rho(\mathbf{r}, \mathbf{r}', t) &= \\ &\left[\hat{h}_{\text{KS}}(\mathbf{r}, t) - \frac{i}{2}\gamma M^2 - \left(\hat{h}_{\text{KS}}(\mathbf{r}', t) + \frac{i}{2}\gamma M^2 \right) \right] \rho(\mathbf{r}, \mathbf{r}', t), \end{aligned} \quad (24)$$

where M follows from (??). Next, we express $\rho(\mathbf{r}, \mathbf{r}', t)$ in terms of a representation of N orthonormal basis functions $\tilde{\varphi}_j$,⁷⁸

$$\rho(\mathbf{r}, \mathbf{r}', t) = \sum_{j=1}^N \tilde{\varphi}_j(\mathbf{r}, t) \tilde{\varphi}_j^*(\mathbf{r}', t). \quad (25)$$

Inserting this representation into (??) yields

$$\begin{aligned} \sum_{j=1}^N \tilde{\varphi}_j^*(\mathbf{r}', t) [i\partial_t - \hat{h}_{\text{KS}}(\mathbf{r}, t)] \tilde{\varphi}_j(\mathbf{r}, t) &= \\ \sum_{j=1}^N \{ \tilde{\varphi}_j^*(\mathbf{r}, t) [i\partial_t - \hat{h}_{\text{KS}}(\mathbf{r}', t)] \tilde{\varphi}_j(\mathbf{r}', t) \}^* & \end{aligned} \quad (26)$$

for the case without dissipation ($\gamma = 0$). In the limit $\gamma = 0$ a single-particle representation can be obtained by introducing the time-dependent matrix

$$C_{jj'}(t) = \langle \tilde{\varphi}_j(t) | i\partial_t - \hat{h}_{\text{KS}}(\mathbf{r}, t) | \tilde{\varphi}_{j'}(t) \rangle. \quad (27)$$

Equation (??) demonstrates that the matrix $C_{jj'}(t)$ is Hermitian (see also Ref. ⁷⁸) and, therefore, can be diagonalized. Based on this finding, we assume that $\{\tilde{\varphi}_j(\mathbf{r}, t)\}$ is the diagonal basis, without loss of generality, and that it fulfills the eigenvalue equation

$$[i\partial_t - \hat{h}_{\text{KS}}(\mathbf{r}, t)] \tilde{\varphi}_j(t) = \varepsilon_j(t) \tilde{\varphi}_j(t) \quad (28)$$

with real eigenvalues $\varepsilon_j(t)$. Next, we consider the case which includes dissipation. For $\gamma \neq 0$ we can introduce in a similar way a matrix $D_{jj'}(t)$ by

$$\begin{aligned} D_{jj'}(t) &= \left\langle \tilde{\varphi}_j(t) \left| i\partial_t - \left(\hat{h}_{\text{KS}}(\mathbf{r}, t) - \frac{i}{2} \gamma M^2 \right) \right| \tilde{\varphi}_{j'}(t) \right\rangle \\ &= C_{jj'}(t) + \frac{i}{2} \gamma M^2 \langle \tilde{\varphi}_j(t) | \tilde{\varphi}_{j'}(t) \rangle, \end{aligned} \quad (29)$$

which includes the dissipative term. $D_{jj'}(t)$ contains the Hermitian contribution $C_{jj'}(t)$ and an anti-Hermitian part $\frac{i}{2} \gamma M^2 \langle \tilde{\varphi}_j(t) | \tilde{\varphi}_{j'}(t) \rangle$. Since our dissipation operator is proportional to a unit operator, the matrix $D_{jj'}(t)$ also remains diagonal in the basis $\{\tilde{\varphi}_j(\mathbf{r}, t)\}$. The eigenvalues $\varepsilon_j(t)$ of $D_{jj'}(t)$ differ from the ones of $C_{jj'}(t)$ by a constant shift in the imaginary part,

$$\varepsilon_j(t) = \varepsilon_j(t) + \frac{i}{2} \gamma M^2. \quad (30)$$

We can set

$$\tilde{\varphi}_j(t) = \exp \left\{ -i \int_{t_0}^t \varepsilon_j(\tau) d\tau \right\} \varphi_j^{\text{aux}}(t) \quad (31)$$

to obtain the set of single-particle equations

$$i\partial_t\varphi_j^{\text{aux}}(t) = \hat{h}_{\text{KS}}\varphi_j^{\text{aux}}(t) - \frac{i}{2}\gamma M^2\varphi_j^{\text{aux}}(t). \quad (32)$$

Note that due to the dissipation, the orbitals $\varphi_j^{\text{aux}}(t)$ do not stay normalized during the time-evolution.

In summary, we have thus demonstrated that the single particle equations in (??) are equivalent to the set of equations (??) when the operator \hat{s}_i is inserted.

B Details of the model system

To guarantee a transparent analysis of the coupling and energetic arrangement we chose sodium dimers as well-accepted model molecules.^{75,79} The Na dimer exhibits strong dipolar character and the electronic structure can easily be modified by bond-length variations (the experimental bond length is 5.78 Bohr). All sodium dimers are aligned along the z -axis according to the setup of 1 and their centers of mass are in the x - y -plane. In the following we discuss the electronic-structure and coupling properties of our model system.

B.1 Single molecule electronic structure

First, we discuss the electronic structure of one dimer, i.e., one subsystem in the ring. We start with Na_2 at the experimental bond length. For excitations oriented along the bond axis, Na_2 is almost a single level atom as there is one prominent excitation at ca. 2.1 eV and a second excitation at 4.1 eV with notably smaller oscillator strength. The excitation energy of the one prominent peak can be calculated as a function of the bond length in two different ways: either from straightforward TDDFT for a dimer with changed bond length, or in a supersystem setup with two dimers (see C). We used both methods and found reasonable agreement. The upper panel of 6 shows that bond length changes of the order of 1 Bohr induce excitation-energy changes of about 0.25 eV.

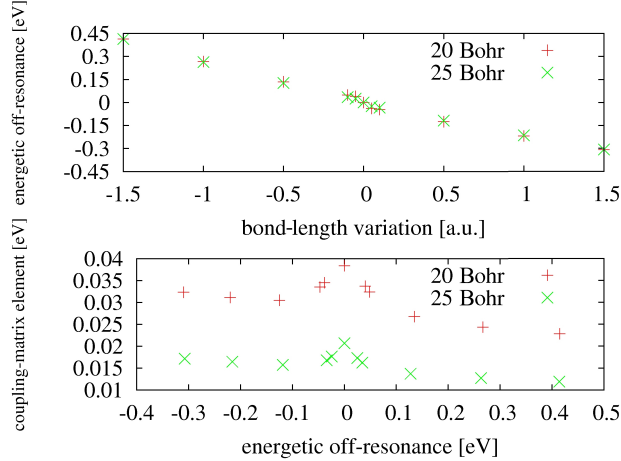


Figure 6: Upper panel: Excitation energy (energetic off-resonance) of Na_2 as a function of the bond length as computed in the supersystem calculation explained in C. Lower panel: Coupling-matrix element calculated in a supersystem of two Na_2 as a function of the energetic off-resonance of one of the dimers.

B.2 Resonant and off-resonant coupling

Second, we study the coupling between two neighboring molecules. Here, we address two influencing factors, namely the distance between the dimers and the energetic arrangement determined by the dimer bond length. The distance dependence of the coupling-matrix element in a resonant situation with sodium dimers of equal bond length was already investigated in an earlier work.⁷⁵ For distances above 25 Bohr, the coupling is of dipole-dipole type, whereas clear deviations from the dipole-dipole character can be observed for smaller distances.

In an off-resonant coupling situation between isolated excited states, a similar two-level picture⁸¹ as in the resonant case⁷⁵ can be used to determine the coupling-matrix element. In analogy to the resonant case the coupling strength can be extracted from the dipole moment of separate system parts (for details, see C). The coupling-matrix element as a function of the energetic off-resonance of the excitation energy of one of the dimers is shown in the lower panel of 6. In the range that we investigated, the coupling-matrix element decreases with increasing excitation energy. The coupling strength peaks at the resonant coupling situation, and the resonant coupling is about 1.4 times larger than the typical off-resonant coupling.

C Off-resonant oscillation in the time-dependent dipole moment

In this appendix we briefly explain how the coupling strength and the energetic off-resonance manifest in the time-dependent dipole moment for a system of one donor molecule D and one acceptor molecule A. The resonant coupling case was already discussed in Ref.⁷⁵ Our considerations employ a two-state model⁸¹ based on the assumption that the wave function of the total system can be separated into D and A parts due to negligible electronic overlap between D and A. Initially, the acceptor is in its ground state denoted by $|A\rangle$ and the donor is in an excited state $|D^*\rangle$. This corresponds to an initial product state $|D^*A\rangle = |D^*\rangle|A\rangle = |1\rangle$. The final wave function corresponds to the inverse situation, $|DA^*\rangle = |2\rangle$. Both states are characterized by their eigenvalues E_1 and E_2 , respectively. We measure energetic off-resonances by the parameter

$$\Delta E = \frac{1}{2}(E_1 - E_2). \quad (33)$$

The coupling between $|1\rangle$ and $|2\rangle$ is mediated by the Coulomb interaction \hat{V}_C . It leads to the coupling-matrix element

$$V = \langle DA^* | \hat{V}_C | D^*A \rangle. \quad (34)$$

The time evolution of the two-state system with initial state $|\Psi(0)\rangle = |1\rangle$ is given by

$$|\Psi(t)\rangle = a_1(t)|1\rangle + a_2(t)|2\rangle \quad (35)$$

with the coefficients $a_1(t)$ and $a_2(t)$,⁸²

$$\begin{aligned} |a_1(t)|^2 &= B + A \cos^2\left(\sqrt{V^2 + \Delta E^2}t\right), \\ |a_2(t)|^2 &= A \sin^2\left(\sqrt{V^2 + \Delta E^2}t\right), \end{aligned} \quad (36)$$

where $A = \frac{V^2}{V^2 + \Delta E^2}$ and $B = \frac{\Delta E^2}{V^2 + \Delta E^2}$. This time evolution of the coefficients corresponds to an in-

complete oscillation with beat frequency $\omega_{\text{beat}} = \sqrt{V^2 + \Delta E^2}$ that depends on the coupling between the initial and the final state as well as the energetic off-resonance: The occupation probability of the initial state varies around B with amplitude A , while the occupation probability of the final state oscillates with amplitude A around zero.

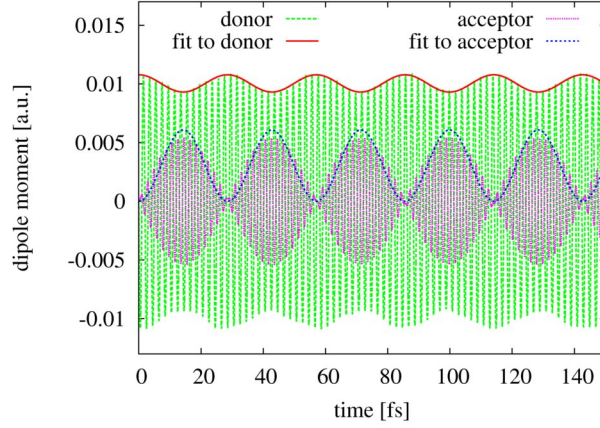


Figure 7: Donor and acceptor dipole moment (z -component) in a setup of two Na_2 , where the bond length of the acceptor Na_2 is reduced by 0.5 Bohr compared to the experimental bond length. We performed fits to the envelope of the oscillation according to the model discussed in the text.

The time-dependent dipole moment $\mathbf{d}^A(t) = \langle \Psi(t) | \hat{\mathbf{r}}^A | \Psi(t) \rangle$ of the acceptor, where we evaluate the dipole operator $\hat{\mathbf{r}}^A$ in the space of the acceptor only, can be calculated as

$$\mathbf{d}^A(t) = |a_1(t)|^2 \langle A | \hat{\mathbf{r}}^A | A \rangle + |a_2(t)|^2 \langle A^* | \hat{\mathbf{r}}^A | A^* \rangle. \quad (37)$$

Here, we exploited the orthogonality of $|D\rangle$ and $|D^*\rangle$. If the static dipole moment $\langle A | \hat{\mathbf{r}}^A | A \rangle$ of A vanishes, (37) simplifies to

$$\mathbf{d}^A(t) = |a_2(t)|^2 \langle A^* | \hat{\mathbf{r}}^A | A^* \rangle. \quad (38)$$

Under the assumption that the static donor dipole moment vanishes, the donor time-dependent dipole moment reads

$$\mathbf{d}^D(t) = |a_1(t)|^2 \langle D^* | \hat{\mathbf{r}}^D | D^* \rangle. \quad (39)$$

Thus, the resonance oscillation of the coefficients can be observed in the time evolution of the

dipole moments $\mathbf{d}^A(t)$ and $\mathbf{d}^D(t)$. In principle, both (??) and (??) can be used to determine the coupling-matrix element V . Of special importance is (??) together with (??), because a fit to the absolute values of the extrema of the k -th component of the donor dipole moment time evolution provides Ap_k , Bp_k , and ω_{beat} , where $p_k = \langle \mathbf{D}^* | \hat{r}_k^D | \mathbf{D}^* \rangle$. It can be used to determine V , ΔE , and p_k . One obtains

$$V = \sqrt{\frac{Ap_k}{Ap_k + Bp_k}} \omega_{\text{beat}} \quad (40)$$

and

$$\Delta E = \sqrt{\frac{Bp_k}{Ap_k + Bp_k}} \omega_{\text{beat}}. \quad (41)$$

A typical time evolution of the z -component of the acceptor and donor dipole moments of our model system is depicted in 7 together with our fits to the envelopes. The two-level model qualitatively fits to the observed dipole oscillation of the off-resonant, coupled system of two molecules. However, the dipole moment envelopes do not perfectly follow the \sin^2 - and \cos^2 -shape. We understand these deviations as a consequence of the coupled system not being perfectly separable into D and A parts, as was assumed in the model. Furthermore, although the second excitation of Na_2 with polarization in z -direction is energetically far off and carries notably smaller oscillator strength, Na_2 is not a perfect single level system, and therefore the system of two sodium dimers does not perfectly match the two-level model. Nevertheless, our approach provides a tool to determine the coupling V and the energetic off-resonance ΔE with reasonable accuracy. The validity of the model can be checked by comparing the ΔE thus obtained to TDDFT excitation energies for a single sodium dimer with changed bond length. We find good agreement and, therefore, assume reasonable quality of the coupling-matrix element results of 6.

References

- (1) Kühlbrandt, W. Photosynthesis - Many Wheels Make Light Work. *Nature* **1995**, 374, 497-498
- (2) Cheng, Y.-C.; Fleming, G.R. Dynamics of Light Harvesting in Photosynthesis. *Annu. Rev.*

- Phys. Chem.* **2009**, 60, 241-262
- (3) Ritz, T.; Damjanović, A.; Schulten, K. The Quantum Physics of Photosynthesis. *Chem. Phys. Chem.* **2002**, 3, 243-248
- (4) Fleming, G. R.; Scholes, G. D. Physical Chemistry - Quantum mechanics for Plants. *Nature* **2004**, 431, 256-257
- (5) Rebentrost, P.; Mohseni, M.; Aspuru-Guzik, A. Role of Quantum Coherence and Environmental Fluctuations in Chromophoric Energy Transport. *J. Phys. Chem. B* **2009**, 113, 9942-9947
- (6) Olaya-Castro, A.; Scholes, G. D. Energy transfer from Forster-Dexter Theory to Quantum Coherent Light-Harvesting. *Int. Rev. Phys. Chem.* **2011**, 49-77
- (7) Engel, G.S.; Calhoun, T.R.; Read, E.L.; Ahn, T.-K.; Mancal, T.; Cheng, Y.-C.; Blankenship, R. E.; Fleming, G.R. Evidence for Wavelike Energy Transfer Through Quantum Coherence in Photosynthetic Systems. *Nature* **2007**, 446, 782-786
- (8) Fleming, G. R.; Schlau-Cohen, G. S.; Amarnath, K.; Zaks, J. Design Principles of Photosynthetic Light-Harvesting. *Faraday Discuss.* **2012**, 155, 27-41
- (9) Strümpfer, J.; Şener, M.; Schulten, K. How Quantum Coherence Assists Photosynthetic Light-Harvesting. *J. Phys. Chem. Lett.* **2012**, 3, 536-542
- (10) Turner, D. B.; Wilk, K. E.; Curmi, P. M. G.; Scholes, G. D. Comparison of Electronic and Vibrational Coherence Measured by Two-Dimensional Electronic Spectroscopy. *J. Phys. Chem. Lett.* **2011**, 2, 1904-1911
- (11) Yuen-Zhou, J.; Krich, J.J.; Aspuru-Guzik, A. A Witness for Coherent Electronic vs Vibronic-Only Oscillations in Ultrafast Spectroscopy. *J. Chem. Phys.* **2012**, 136, 234501-1-234501-11

- (12) Brédas, J.-L.; Silbey, R.; CHEMISTRY Excitons Surf Along Conjugated Polymer Chains. *Science* **2009**, 323, 348-349
- (13) Collini, E.; Scholes, G. D. Coherent Intrachain Energy Migration in a Conjugated Polymer at Room Temperature. *Science* **2009**, 323, 369-373
- (14) Scholes, G. D.; Flemming, G. R.; Olaya-Castro, A.; van Grondelle, R. Lessons from Nature about Solar Light Harvesting. *Nature Chem.* **2011**, 3 763-774
- (15) Harel, E. Long Range Excitonic Transport in a Biomimetic System Inspired by the Bacterial Light-Harvesting Apparatus. *J. Chem. Phys.* **2012** 136, 174104-1-174104-10
- (16) Jang, S.; Jung, Y. J.; Silbey, R. J.; Nonequilibrium Generalization of Forster-Dexter Theory for Excitation Energy Transfer. *Chem. Phys.* **2002**, 275, 319-332
- (17) Yang, M.; Fleming, G.R. Influence of Phonons on Exciton Transfer Dynamics: Comparison of the Redfield, Forster, and Modified Redfield Equations. *Chem. Phys.* **2002**, 275, 355-372
- (18) Jang, S.; Cheng, Y.-C.; Reichnam, D. R.; Eaves, J. D. Theory of Coherent Resonance Energy Transfer. *J. Chem. Phys.* **2008**, 129, 101104
- (19) Ishizaki, A.; Fleming, G. R. Unified Treatment of Quantum Coherent and Incoherent Hopping Dynamics in Electronic Energy Transfer: Reduced Hierarchy Equation Approach. *J. Chem. Phys.* **2009** 130, 234110-1-234110-10
- (20) Ishizaki, A.; Fleming, G. R. On the Adequacy of the Redfield Equation and Related Approaches to the Study of Quantum Dynamics in Electronic Energy Transfer. *J. Chem. Phys.* **2009**, 130, 234111-1-234111-8
- (21) Olšina, J.; Mančal, T. J. Electronic Coherence Dephasing in Excitonic Molecular Complexes: Role of Markov and Secular Approximations. *Mol. Model.* **2010** 16, 1765-1778.

- (22) Kolli, A.; Nazir, A.; Olaya-Castro, A. Electronic Excitation Dynamics in Multichromophoric Systems Described Via a Polaron-Representation Master Equation. *J. Chem. Phys.* **2011**, 135, 154112-1-154112-13
- (23) Di Ventra, M. D'Agosta, R., Stochastic Time-Dependent Current-Density-Functional Theory. *Phys. Rev. Lett.* **98** **2007**, 226403-1-226403-4
- (24) D'Agosta R.; Di Ventra, M., Stochastic Time-Dependent Current-Density-functional Theory: A Functional Theory of Open Quantum Systems. *Phys. Rev. B* **2008** 78, 165105-1-165105-16
- (25) Appel, H.; Di Ventra, M. Stochastic Quantum Molecular Dynamics. *Phys. Rev. B* **2009** 80, 212303-1-212303-4
- (26) Appel, H.; Di Ventra, M. Stochastic Quantum Molecular Dynamics for Finite and Extended Systems. *Chem. Phys.* **2011**, 391, 27-36
- (27) Biele, R.; D'Agosta, R. A Stochastic Approach to Open Quantum Systems. *J. Phys.: Condens. Matter* **2012**, 24, 273201-1-273201-23
- (28) H. Appel, in *Fundamentals of Time-Dependent Density Functional Theory*, Chap. 11 (Springer Verlag, Berlin, 2012).
- (29) Bushong, N.; Di Ventra, M. The Decay of Excited He from Stochastic Density-Functional Theory: A Quantum Measurement Theory Interpretation. *J. Phys.: Condens. Matter* **2008**, 20, 395214-1-395214-4
- (30) Pershin, Yu. V.; Dubi, Y., Di Ventra, M. Effective Single-Particle Order-N Scheme for the Dynamics of Open Noninteracting Many-Body Systems. *Phys. Rev. B* **2008**, 78, 054302-1-054302-8
- (31) R. D'Agosta and M. Di Ventra, Foundations of Stochastic Time-Dependent Current-Density

- Functional Theory for Open Quantum Systems: Potential Pitfalls and Rigorous Results. *Phys. Rev. B* **2013** 87, 155129-1-155129-7
- (32) Runge, E.; Gross, E.K.U. Density-Functional Theory for Time-Dependent Systems. *Phys. Rev. Lett.* **1984**, 52, 997-1000
- (33) Gross, E. K. U.; Dobson, J. F.; Petersilka, M. in *Density Functional Theory*, edited by R. F. Nalewajski, Top. Curr. Chem. (Springer, Berlin, 1996), Vol. 181, p. 81.
- (34) Yabana, K.; Bertsch, G.F. Time-Dependent Local-Density Approximation in Real Time. *Phys. Rev. B* **1996** 54, 4484-4487
- (35) Yabana, K.; Bertsch, G. F. Time-Dependent Local-Density Approximation in Real Time: Application to Conjugated Molecules. *Int. J. Quantum Chem.* **1999**, 75, 55-66
- (36) Marques, M. A. L.; Gross, E.K.U. Time-Dependent Density Functional Theory. *Annu. Rev. Phys. Chem.* **2004**, 55, 427-455
- (37) Marques, M. A. L.; Maitra, N. T. ; Nogueira, F. M. S. ; Gross, E. K. U. ; Rubio, A. (Eds.), *Fundamentals of Time-Dependent Density Functional Theory (Lecture Notes in Physics)* (Springer Verlag, Berlin, 2012).
- (38) Neugebauer, J. Couplings Between Electronic Transitions in a Subsystem Formulation of Time-Dependent Density Functional Theory. *J. Chem. Phys.* **2007**, 126, 134116-1-134116-12
- (39) Yanai, T., Tew, D. P.; Handy, N. C. A New Hybrid Exchange&Correlation Functional Using the Coulomb-Attenuating Method (CAM-B3LYP). *Chem. Phys. Lett.* **2004**, 393, 51-57
- (40) J.-D. Chai and M. Head-Gordon, Systematic Optimization of Long-Range Corrected Hybrid Density Functionals. *J. Chem. Phys.* **2008**, 128, 084106-1-084106-15

- (41) Peach, M. J. G.; Benfield, P.; Helgaker, T.; Tozer, D. J. Excitation Energies in Density Functional Theory: An Evaluation and a Diagnostic Test. *J. Chem. Phys.* **2008** 128, 044118-1-044118-8
- (42) Stein, T.; Kronik, L.; Baer, R. Reliable Prediction of Charge Transfer Excitations in Molecular Complexes Using Time-Dependent Density Functional Theory. *J. Am. Chem. Soc.* **2009**, 131, 2818-2820
- (43) Karolewski, A.; Armiento, R.; Kümmel, S. Polarizabilities of Polyacetylene from a Field-Counteracting Semilocal Functional. *J. Chem. Theory Comput.* **2009**, 5, 712-718
- (44) Karolewski, A.; Stein, T.; Baer, R.; Kümmel, S. Tailoring the Optical Gap in Light-Harvesting Molecules. *J. Chem. Phys.* **2011**, 134, 151101-1-151101-4
- (45) Hofmann, D.; Körzdörfer, T.; Kümmel, S. Kohn-Sham Self-Interaction Correction in Real Time *Phys. Rev. Lett.* **2012**, 108, 146401-1-146401-5
- (46) Hofmann, D.; Kümmel, S. Self-interaction Correction in a Real-Time Kohn-Sham scheme: Access to Difficult Excitations in Time-Dependent Density Functional Theory. *J. Chem. Phys.* **2012** 137, 064117-1-064117-17
- (47) Kronik, L.; Stein, T.; Refaely-Abramson, S.; Baer, R. Excitation Gaps of Finite-Sized Systems from Optimally Tuned Range-Separated Hybrid Functionals. *J. Chem. Theory Comput.* **2012** 8, 1515-1531
- (48) Hofmann, D.; Kümmel, S. Integer Particle Preference During Charge Transfer in Kohn-Sham Theory. *Phys. Rev. B* **2012** 86, 201109-1-201109-4
- (49) Burke, K.; Car, R.; Gebauer, R. Density Functional Theory of the Electrical Conductivity of Molecular Devices. *Phys. Rev. Lett.* **2005** 94, 146803-1-146803-4
- (50) Yuen-Zhou, J.; Rodríguez-Rosario, C.; Aspuru-Guzik, A. Time-Dependent Current-Density

- Functional Theory for Generalized Open Quantum Systems. *Phys. Chem. Chem. Phys.* **2009** 11, 4509-4522
- (51) Yuen-Zhou, J.; Tempel, D. G.; Rodríguez-Rosario, C.; Aspuru-Guzik, A. Time-Dependent Density Functional Theory for Open Quantum Systems with Unitary Propagation. *Phys. Rev. Lett.* **2010** 104, 043001-1- 043001-4
- (52) Tempel, D. G.; Aspuru-Guzik, A. Relaxation and Dephasing in Open Quantum Systems Time-Dependent Density Functional Theory: Properties of Exact Functionals from an Exactly-Solvable Model System. *Chem. Phys.* **2011** 391, 130-142
- (53) Tempel, D. G.; Watson, M. A.; Olivares-Amaya, R.; Aspuru-Guzik, A. Time-Dependent Density Functional Theory of Open Quantum Systems in the Linear-Response Regime. *J. Chem. Phys.* **2011** 134, 074116-1-074116-17
- (54) Zheng, X.; Yam, C.; Wang, F.; Chen, G. Existence of Time-Dependent Density-Functional Theory for Open Electronic Systems: Time-Dependent Holographic Electron Density Theorem. *Phys. Chem. Chem. Phys.* **2011** 13, 14358-14364
- (55) Tempel, D. G.; Yuen-Zhou, J.; Aspuru-Guzik, A. in *Fundamentals of Time-Dependent Density Functional Theory*, Chap. 10 (Springer Verlag, Berlin, 2012).
- (56) Dalibard, J.; Castin, Y.; Mølmer, K. Wave-Function Approach to Dissipative Processes in Quantum Optics. *Phys. Rev. Lett.* **1992** 68, 580-583
- (57) Gaspard, P.; Nagaoka, M. Non-Markovian Stochastic Schrodinger Equation. *J. Chem. Phys.* **1999** 111, 5676-5690
- (58) Breuer, H.-P.; Petruccione, F. *The Theory of Open Quantum Systems* (Clarendon Press, Oxford, 2006).
- (59) van Kampen, N. G. *Stochastic Processes in Physics and Chemistry*, third ed. (Elsevier, Amsterdam, 2007).

- (60) Weiss, U. *Quantum Dissipative Systems*, third ed. (World Scientific, Singapore, 2008).
- (61) van Leeuwen, R. Mapping from Densities to Potentials in Time-Dependent Density-Functional Theory. *Phys. Rev. Lett.* **1999**, 82, 3863-3866
- (62) Vignale, G. Mapping from Current Densities to Vector Potentials in Time-Dependent Current Density Functional Theory. *Phys. Rev. B* **2004**, 70, 201102(R)-1-201102(R)-4
- (63) D'Agosta, R.; Vignale, G. Non-V-Representability of Currents in Time-Dependent Many-Particle Systems. *Phys. Rev. B* **2005**, 71, 245103-1-245103-6
- (64) Hofmann-Mees, D. Charge and Excitation-Energy Transfer in Time-Dependent Density Functional Theory. PhD-Thesis, University of Bayreuth **2012**
- (65) Körzdörfer, T.; Kümmel, S. Single-Particle and Quasiparticle Interpretation of Kohn-Sham and Generalized Kohn-Sham Eigenvalues for Hybrid Functionals. *Phys. Rev. B* **2010**, 82, 155206-1-155206-9
- (66) Puschnig, P.; Berkebile, S.; Fleming, A. J.; Koller, G.; Emtsev, K.; Seyller, T.; Riley, J. D.; Ambrosch-Draxl, C.; Netzer, F. P.; Ramsey, M. G. Reconstruction of Molecular Orbital Densities from Photoemission Data. *Science* **2009**, 326, 702-706; Puschnig, P.; Reinisch, E.-M.; Ules, T.; Koller, G.; Soubatch, S.; Ostler, M.; Romaner, L.; Tautz, F.S.; Ambrosch-Draxl, C.; Ramsey, M.G. Orbital Tomography: Deconvoluting Photoemission Spectra of Organic Molecules. *Phys. Rev. B* **2011**, 84, 235427-1-235427-8
- (67) Dauth, M.; Körzdörfer, T.; Kümmel, S.; Zirotti, J.; Wiessner, M.; Schöll, A.; Reiner, F.; Arita, M.; Shimada, K. Orbital Density Reconstruction for Molecules. *Phys. Rev. Lett.* **2011**, 107, 193002-1-193002-5
- (68) Gardiner, C. W.; Parkins, A. S.; Zoller, P. Wave-Function Quantum Stochastic Differential Equations and Quantum-Jump Simulation Methods. *Phys. Rev. A* **1992**, 46, 4363-4381

- (69) Breuer, H.-P.; Petruccione, F. Stochastic Dynamics of Quantum Jumps. *Phys. Rev. E* **1995**, 52, 428-441
- (70) Mundt, M.; Kümmel, S. Photoelectron Spectra of Anionic Sodium Clusters from Time-Dependent Density-Functional Theory in Real Time. *Phys. Rev. B* **2007**, 76, 035413-1-035413-8
- (71) Kronik, L.; et al. PARSEC - the Pseudopotential Algorithm for Real-Space Electronic Structure Calculations: Recent Advances and Novel Applications to Nano-Structures. *Phys. status solidi B* **2006**, 243, 1063-1079
- (72) Kümmel, S.; Andrae, K.; Reinhard, P.-G. Collectivity in the Optical Response of Small Metal Clusters. *Appl. Phys. B* **2001**, 73, 293-297
- (73) Castro, A.; Appel, H.; Oliveira, M.; Rozzi, C.A.; Andrade, X.; Lorenzen, F.; Marques, M.A.L.; Gross, E.K.U.; Rubio, A. Octopus: A Tool for the Application of Time-Dependent Density Functional Theory. *Phys. Stat. Sol. B* **2006**, 243, 2465-2488
- (74) Thiele, M.; Kümmel, S.; Photoabsorption Spectra from Adiabatically Exact Time-Dependent Density-Functional Theory in Real Time. *Phys. Chem. Chem. Phys.* **2009**, 11, 4631-4639
- (75) Hofmann, D.; Körzdörfer, T.; Kümmel, S. Energy Transfer and Förster's Dipole Coupling Approximation Investigated in a Real-Time Kohn-Sham Scheme. *Phys. Rev. A* **2010**, 82, 012509-1-012509-9
- (76) Scholes, G. D. Long-Range Resonance Energy Transfer In Molecular Systems. *Annu. Rev. Phys. Chem.* **2003**, 54, 57-87
- (77) König, C.; Neugebauer, J. Quantum Chemical Description of Absorption Properties and Excited-State Processes in Photosynthetic Systems. *Chem. Phys. Chem.* **2012**, 13, 386-425

- (78) Wong, C.-Y.; Tang, H. H. K.; Dynamics of Nuclear Fluid. V. Extended Time-Dependent Hartree-Fock Approximation Illuminates the Approach to Thermal Equilibrium. *Phys. Rev. C* **1979**, 20, 1419–1452
- (79) All calculations are based on the local density approximation (LDA). We used real-space grids with a grid spacing of 0.7 Bohr, a propagation time step of 0.001 fs, and norm conserving LDA pseudopotentials of Troullier-Martins⁸⁰ type (core cut-off radius $r_c(\text{Na})=3.09$ Bohr).
- (80) Troullier, N.; Martins, J. L.; Efficient Pseudopotentials for Plane-Wave Calculations. *Phys. Rev. B* **1991**, 43, 1993–2006
- (81) Neugebauer, J. Photophysical Properties of Natural Light-Harvesting Complexes Studied by Subsystem Density Functional Theory. *J. Phys. Chem. B* **2008**, 112, 2207–2217
- (82) C. Cohen-Tannoudji, B. Diu, and F. Laloë, *Quantenmechanik Band 1* (Walter de Gruyter, 2009), p. 374.

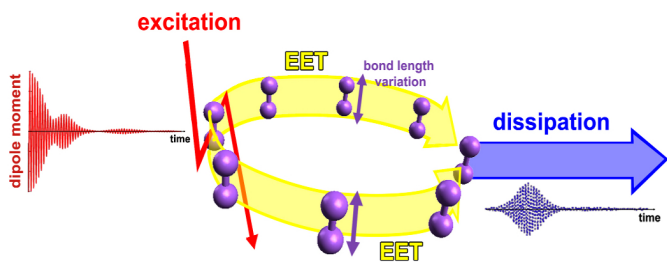


Table of Contents figure: Illustration of a scheme to compute excitation energy transfer